Published in final edited form as:
Nat Neurosci. 2007 February ; 10(2): 215–223. doi:10.1038/nn1828.

SHARPENED COCHLEAR TUNING IN A MOUSE WITH A GENETICALLY MODIFIED TECTORIAL MEMBRANE

Ian J. Russell[*], **P. Kevin Legan**, **Victoria A. Lukashkina**, **Andrei N. Lukashkin**, **Richard J. Goodyear**, and **Guy. P Richardson**[*]
School of Life Sciences, University of Sussex, Falmer, Brighton, BN1 9QG, UK

Abstract

Frequency tuning in the cochlea is determined by the passive mechanical properties of the basilar membrane and active feedback from the outer hair cells, sensory-effector cells that detect and amplify sound-induced basilar membrane motions. The sensory hair bundles of the outer hair cells are imbedded in the tectorial membrane, a sheet of extracellular matrix that overlies the cochlea's sensory epithelium. The tectorial membrane contains radially-organised collagen fibrils imbedded in an unusual, striated-sheet matrix formed by two glycoproteins, Tecta and Tectb. In *Tectb*$^{-/-}$ mice the structure of the striated-sheet matrix is disrupted. Although these mice have a low-frequency hearing loss, basilar membrane and neural tuning are both significantly enhanced in the high-frequency regions of the cochlea, with little loss in sensitivity. These findings can be attributed to a reduction in the acting mass of the tectorial membrane, and reveal a novel role for this structure in controlling interaction along the cochlea.

The cochlea is the mammalian organ of hearing, a sensory organ that detects sound stimuli and converts them into electrical signals. It is a coiled, fluid-filled tube that is divided along its length by the basilar membrane, a strip of collagen-based extracellular matrix. The basilar membrane is graded in stiffness along the length of the cochlea and vibrates in response to sound induced movements of the cochlear fluids[1, 2]. These vibrations are detected by hair cells located in the organ of Corti, a sensory epithelium that sits upon and runs along one edge of the basilar membrane. There are two types of hair cells in the organ of Corti, the inner and outer hair cells (IHCs and OHCs respectively). The mechanosensory hair bundles of these cells project up from the sensory epithelium's apical surface, the reticular lamina, towards the overlying tectorial membrane, a unique, ribbon-like extracellular matrix structure that contains different types of collagen and three non-collagenous glycoproteins that are only expressed at high levels in the inner ear; α-tectorin (Tecta), β-tectorin (Tectb) and otogelin[3].

The hair bundles of the OHCs are firmly imbedded in the tectorial membrane, and are stimulated by the shear motion that develops between the tectorial membrane and the reticular lamina in response to sound-induced vibrations of the basilar membrane. The basilar membrane is very sharply tuned to different frequencies along its length, and the sharpness of tuning depends not only on the membrane's passive mechanical properties but also upon active feedback from the OHCs, sensory-effector cells that detect and influence mechanical interactions between the tectorial membrane and the reticular lamina [4]. OHCs deliver electromechanical feedback to the cochlea at frequencies close to the characteristic frequency of their location on the basilar membrane. OHC feedback amplifies responses to

[*]Correspondence should be addressed to I.R. (I.J.Russell@sussex.ac.uk) or G.R. (G.P.Richardson@sussex.ac.uk)..

COMPETING INTERESTS STATEMENT The authors declare that they have no competing financial interests.

Europe PMC Funders Author Manuscripts

low-level characteristic frequency tones, compresses them at high-levels, and determines the large dynamic range, exquisite sensitivity and frequency tuning of the cochlea[2, 5]. The IHCs appear to be purely sensory[4]. Their hair bundles are free standing and not directly imbedded in the tectorial membrane. *In vivo* measurements of IHC receptor potentials[6, 7] indicate that their hair bundles respond through fluid coupling to the velocity of the basilar membrane at low frequencies. *In vitro* measurements of hair bundle motion reveal that the hair bundles of IHCs are stimulated by relative shear between the reticular lamina and the tectorial membrane, probably as a consequence of complex fluid movements in the narrow subtectorial space[8, 9, 10].

Due to its inaccessible location and susceptibility to changes in its unique ionic environment[11], the precise role played by the tectorial membrane in hearing has been hard to determine. The function of the tectorial membrane has, however, been the subject of a number of theories[12-16]. Recent studies with *in vitro* models[9, 10, 17 -20] have provided invaluable information and evidence[17, 18] for the radial resonant properties of the tectorial membrane originally proposed by Zwislocki[13] and Allen[12]. Although evidence for a second resonator has not been seen in most *in vivo* studies of basilar membrane motion[5], it has been observed in the basal, high-frequency cochlear turns of the mustached bat and mice[19-22] as predicted from *in vitro* measurements of tectorial membrane stiffness, which indicate the tectorial membrane has a stiffness comparable to that of the basilar membrane loaded with the organ of Corti[23]. If the tectorial membrane and the organ of Corti provide a significant load on the basilar membrane, they will be able to affect the macromechanics and the motion of the basilar membrane [24,25].

The tectorins, Tecta and Tectb, are proteins that are exclusively restricted, within the cochlear duct, to the tectorial membrane and are thus ideal targets for the selective and specific transgenic manipulation of this matrix. Studies with mice carrying a functional null mutation in *Tecta* (*Tecta*$^{\Delta ENT/\Delta ENT}$)[21] have confirmed the *in vitro* findings[17,18], showing that the tectorial membrane has a resonance *in vivo* and acts as an inertial load against which OHCs can interact at the characteristic frequency of the basilar membrane. In addition, these mice have revealed that the tectorial membrane plays a key role in ensuring OHCs are displacement coupled, operating in the most sensitive region of their transfer functions, and therefore able to deliver feedback to the basilar membrane with optimal gain and timing[21]. Mice heterozygous for a missense mutation in *Tecta* (*Tecta*$^{Y1870C/+}$) have provided evidence that the tectorial membrane also plays an essential role in driving the IHCs, specifically at their characteristic frequency [22].

It is widely understood that frequency resolution in the cochlea is determined by the travelling wave of the basilar membrane and its enhancement through cochlear feedback[2]. Here we report that in the frequency region of the cochlea above 20 kHz, the loss of Tectb from the tectorial membrane causes an increase in the sharpness of cochlear tuning with little or no loss in sensitivity. This novel role for the tectorial membrane in determining the frequency resolution of the cochlea can be attributed to a reduction in the strength of longitudinal mechanical coupling within the tectorial membrane.

RESULTS

Loss of striated-sheet matrix in *Tectb*$^{-/-}$ mutant mice

The core of the tectorial membrane is composed of radially-oriented collagen fibril bundles that are imbedded in sheets of non-collagenous matrix with a striated appearance[26]. Striated-sheet matrix is completely absent from the residual, detached tectorial membranes of mice with a functional null mutation in *Tecta*[21], and the structure of this matrix is largely unaffected in otogelin null mutant mice[27] indicating Tecta is a major constituent of this non-

collagenous component of the tectorial membrane. We used gene targeting in embryonic stem cells to delete exons 1-4 of the *Tectb* gene (Fig.1a,b). Although a truncated mRNA was still expressed from the remaining exons (Fig. 1c), Tectb was not detected in the tectorial membranes or epithelia of mice homozygous for this deletion (Figs. 1d and 2a,b). The global distributions of Tecta and otogelin in the tectorial membrane were unaffected by the mutation (Fig. 2c–f). The tectorial membrane remained attached to the spiral limbus in homozygous $Tectb^{-/-}$ mutant mice and extended laterally across the surface of the organ of Corti, as in wild type mice or in mice heterozygous for this mutation (Fig. 2g–j). The matrix of the tectorial membrane was less dense in Toluidin blue-stained sections of both the apical, low-frequency and basal, high-frequency coils of the cochlea in the $Tectb^{-/-}$mutant mice (Fig. 2g–j). The cross-sectional area of the tectorial membrane in the distal end of the apical cochlear coil of the $Tectb^{-/-}$ mutant mouse was approximately twice that of heterozygous or wild type mice (11544±1130 μm^2 vs. 5278±730 μm^2, $P = 2.46E\text{-}8$) (Fig. 2g,h), but it was not significantly different (1790±352 μm^2 vs. 1845±118 μm^2, $P = 0.72$) in the basal coils (Fig. 2i, j). The thickness of the tectorial membrane in the apical coil of the $Tectb^{-/-}$ mutant was twice that of the heterozygous or wild type mice (72.1±3.5 μm vs. 36.4±1.9 μm, $P = 1.63E\text{-}11$), but the radial width was unchanged (180.4±24.2 μm vs. 172.4±16.2 μm, $P = 0.48$). In the basal coil, neither the thickness (23.9±2.5 μm vs 21.6±2.3 μm, $P = 0.14$) nor the radial width (84.7±10.5 μm vs 87.9±8.9 μm, $P = 0.56$) of the tectorial membrane was significantly different in the $Tectb^{-/-}$ mutant. Analysis of anti-Tecta stained cryosections also indicated there was no difference in the thickness, radial width and cross-sectional area of the tectorial membrane in the basal cochlear coil of $Tectb^{+/-}$ and $Tectb^{-/-}$ mice (not shown). Whilst the tectorial membrane of the $Tectb^{-/-}$ mutant mouse retained a peripheral surrounding mantle composed of a covernet, marginal band and Kimura's membrane in the basal coil, there was a noticeable absence of Hensen's stripe, a longitudinal ridge thought to engage the hair bundles of the inner hair cells (IHCs)[28,29] (Fig. 2i,j inserts; k,l). In the apical end of the apical coil, the marginal band was absent and the tectorial membrane had a markedly frayed peripheral edge in the $Tectb^{-/-}$ mutant (Fig. 2m,n). Analysis of wholemount tectorial membrane preparations indicated that the frayed, disrupted margin extends to a position located 30–40% of the length of the tectorial membrane from its extreme apical end.

Transmission electron microscopy revealed a complete absence of striated-sheet matrix throughout the length of the tectorial membrane in $Tectb^{-/-}$ mutant mice (Fig. 3a,b). Irregular, wavy, 8–10 nm diameter fibrils were found instead between the collagen fibril bundles in the $Tectb^{-/-}$ mutant, and straight fibrils of a similar diameter were observed aligned along and between the individual collagen filaments (Fig. 3b). Scanning electron microscopy indicated that these changes in tectorial membrane morphology did not influence the structure of the underlying hair bundles (Fig. 3c–f). In both the apical (Fig. 3c,d) and basal (Fig. 3e,f) coils of the mature cochlea, the form, orientation and density of the hair bundles on inner and outer hair cells were normal. Scanning electron microscopy also revealed the presence of hair-bundle imprints, the sites of OHC hair-bundle attachment, on the lower surface of the tectorial membrane in both wild type and $Tectb^{-/-}$ mutant mice (Fig. 3g,h). Light microscopy (not shown) indicated the $Tectb^{-/-}$ mutant mice have an identical morphological phenotype on the F1 hybrid backgrounds (CBA/C57, CBA/129 and C57/129).

OHC receptor potentials are unaltered in $Tectb^{-/-}$ mice

We recorded extracellular receptor potentials from within the organ of Corti, very close to the OHCs, in the basal turn of the cochlea (Figs. 4a,b). A stimulus frequency (10 kHz) was chosen as it is above the lower-frequency limit of the mouse cochlea[30], but within the range of frequencies, 2–3 octaves below the characteristic frequency range of the basal turn, over

which the mechanical properties of the tectorial membrane are dominated by its dynamic radial stiffness[14]. Extracellular receptor potentials recorded from wild type mice[21, 22, 31] are typically symmetrical for levels below 70 dB SPL (sound pressure level re 2×10^{-5} Pa) and this was also observed in *Tectb*$^{-/-}$ mutant mice. The symmetry of the receptor potentials followed a general level-dependent pattern, usually becoming negatively asymmetrical for levels below 90 dB SPL, symmetrical between 85–95 dB SPL and positively asymmetrical for levels above this[21, 31]. The magnitudes (Fig. 4b) and phase (not shown) of the extracellular receptor potentials recorded from wild type and *Tectb*$^{-/-}$ mutant mice as functions of SPL were very similar. Assuming the loss of Tectb does not cause a compensatory change in the sensitivity of the hair-cell's mechanotransduction apparatus, these results indicate that the dynamic radial stiffness of the tectorial membrane is unaltered in the high-frequency basal region of the cochlea.

Basilar membrane tuning is sharper in *Tectb*$^{-/-}$ mice

The ability of the ear to resolve sound into individual frequency components is determined largely by the frequency tuning of the basilar membrane [1, 5]. Basilar membrane threshold frequency tuning curves (0.2 nm criterion) were measured from the cochleae of 8 wild type and 8 *Tectb*$^{-/-}$ mutant mice by directing the beam of a laser diode through the round window membrane onto the 53 kHz place of the basilar membrane in the basal turn (Fig. 4a,c). The 53 kHz place is at the same location in wild type and *Tectb*$^{-/-}$ mutant mice, and is 50–100 μm from the 50 kHz location, the lowest frequency region that is just accessible to measurements with the laser interferometer through the round window membrane. For clarity, the error bars for the tuning curves are presented in the negative direction for data from wild type mice, and in the positive direction for data from *Tectb*$^{-/-}$ mutants. The thresholds at the tips of the tuning curves measured in wild type mice and *Tectb*$^{-/-}$ mutant mice were 22.33± 6.23 dB SPL and 33.25 ± 4.72 dB SPL respectively. In *Tectb*$^{-/-}$ mutant mice, basilar membrane vibrations at the characteristic frequency of the recording site were therefore about 10 dB less sensitive than those of wild type mice at the tips of the tuning curves. The bandwidths of tuning curves measured from *Tectb*$^{-/-}$ mutant mice were, however, less broad than those of wild type mice with a mean $Q_{10\ dB}$ (characteristic frequency / bandwidth 10 dB from tip) of 18.9 ± 2.6 (mean ± s.d.) compared with that of 9.6 ± 3.3 for wild type mice. The high and low frequency slopes of wild type tuning curves were 99 dB.octave^{-1} and 187 dB.octave^{-1} respectively, whilst those of *Tectb*$^{-/-}$ mutant mice were 152 dB.octave^{-1} and 314 dB.octave^{-1}. The low-frequency resonance (indicated by the arrow in Fig. 4c) that has been observed in previous measurements from the mouse basilar membrane and attributed to the tectorial membrane [21] was seen only in the tuning curves of wild type mice. The low-frequency tail of the tuning curve from *Tectb*$^{-/-}$ mutant mice was on average less sensitive than that of wild type mice and decreased in sensitivity with a mean slope of 8.2 ± 1.6 dB.octave^{-1}, compared with 14.5 ± 1.4 dB.octave^{-1} for wild type mice ($P < 0.001$), a difference of 6.3 dB/octave from 10 kHz to 53 kHz (lowest curve in Fig. 4c).

Plots of basilar membrane phase (mean ± s.d.) relative to that of the malleus, measured at 70 dB SPL and as a function of stimulus frequency, taken from the 53 kHz place of 4 wild type and 4 *Tectb*$^{-/-}$ mutant mice are shown Fig. 4d. The plots were similar in overall phase delay to phase curves measured from guinea pigs, chinchillae and gerbils[5] but they differed in form with a phase lead of about 270° in the region of the low frequency resonance. In wild type mice this phase lead occured at a frequency that is 3 kHz lower than that in *Tectb*$^{-/-}$ mutant mice. The slope of the phase curve in *Tectb*$^{-/-}$ mutant mice (0.2904 ± 0.0077 octaves.kHz^{-1}) was steeper than that of wild type mice (0.2171 ± 0.0151 octaves.kHz^{-1}) ($P < 0.001$). The curves were, however, coincident close to the characteristic frequency of the measurement place. Differences in the phase of basilar membrane displacement measured at

moderate levels (45 dB SPL, when basilar membrane vibrations are actively amplified) and at high levels (75 dB SPL, when basilar membrane vibrations are largely passive)[5] revealed that basilar membrane phase changed more rapidly with frequency about the characteristic frequency in the *Tectb*$^{-/-}$ mutant mice than it does in wild type mice (Fig. 4e), as would be expected from a system with actively enhanced frequency tuning.

Neural masking tuning curves are sharper in *Tectb*$^{-/-}$ mice

Simultaneous masking neural tuning curves[32] closely resemble the tuning properties of single auditory nerve fibers[33] and are more sharply tuned in *Tectb*$^{-/-}$ mutant mice than in wild type mice (Fig. 5a and Table 1). The low-frequency slope of the tuning curves was almost three times steeper in *Tectb*$^{-/-}$ mice, and the high-frequency slope was almost twice as steep as that of wild type mice. Masking neural tuning curves from the different background strains were not significantly different within the wild type and *Tectb*$^{-/-}$ mutant groups (Fig. 5b), indicating the phenotype was faithfully expressed regardless of the genetic background.

For frequencies within the tuning curve tip, the neural masking and the mechanical tuning curves of wild type mice had similar $Q_{10\ dB}$s. The neural responses of *Tectb*$^{-/-}$ mutant mice were, however, more sharply tuned than the mechanical responses at the tip of the tuning curves and the low-frequency shoulder was very insensitive (Fig. 5a–c and Table 1). A notch of insensitivity is seen in the neural masking frequency tuning[32, 34] curves and in neural tuning curves[16, 33] at the frequency where the tip of the tuning curve meets the tail. In wild type mice, the notch occurred between 1 and 0.26 octaves below the probe frequency. In *Tectb*$^{-/-}$ mutant mice the notch occurred between 0.32 and 0.14 octaves below the probe frequency (Fig. 5d).

Loss of low-frequency cochlear sensitivity in *Tectb*$^{-/-}$ mice

Neural audiograms, based on the detection threshold of the compound action potential (CAP) recorded from the round windows of wild type and *Tectb*$^{-/-}$ mutant mouse cochleae, revealed a distinct low-frequency hearing loss in the *Tectb*$^{-/-}$ mutant mice. For frequencies above ~ 20 kHz, however, neural sensitivities in wild type and *Tectb*$^{-/-}$ mutant mice were very similar. Neural thresholds for frequencies between 20–70 kHz were < 40 dB SPL in the most sensitive mice and have a mean of ~ 50 dB SPL for all measurements reported in this paper (Fig. 5e). The enhanced high-frequency tuning in the *Tectb*$^{-/-}$ mutant mice, therefore, came at the expense of a hearing loss for frequencies below 20 kHz (Fig. 5e).

Cochlear, and in particular OHC, sensitivity can also be assessed non-invasively over the entire frequency range by measuring distortion product otoacoustic emissions (DPOAEs), signals that are generated by OHCs when the cochlea is stimulated by two tones, with the most prominent DPOAE being the 2f1–f2 DPOAE[35]. DPOAEgrams (Fig. 5f) revealed that DPOAEs were generated across the entire 5–60 kHz frequency measurement range in the cochleae of wild type mice, regardless of the level of the primary tones. DPOAEs recorded from *Tectb*$^{-/-}$ mutant mice were, by contrast, frequency-dependent. At low levels only the high-frequency, basal region of the cochlea generated DPOAEs. With increasing levels of the primary tones, and hence increased BM velocity, the region of DPOAE generation extended towards the lower frequencies (Fig. 5f). Even with the highest levels of primaries used in these experiments, DPOAE levels in the frequency region below 20 kHz were 20–30 dB less than those recorded from wild type mice (Fig. 5f).

DISCUSSION

In this study we show that the presence of Tectb, one of the two major non-collagenous glycoproteins of the mammalian tectorial membrane[3], is essential for low-frequency hearing. The loss of the marginal band and the gross enlargement of the tectorial membrane cause a significant loss of cochlear sensitivity for frequencies below 20 kHz. By contrast, the absence of Tectb from the tectorial membrane in the basal, high-frequency region of the cochlea causes little loss in sensitivity and leads to enhanced frequency tuning.

Tecta and Tectb are the major non-collagenous glycoproteins of the mammalian tectorial membrane[3]. Immunofluorescence studies indicate both proteins are, within the cochlear duct, exclusively restricted to the tectorial membrane and distributed uniformly throughout this matrix[3]. In mice with a functional null mutation in *Tecta* (*Tecta*$^{\Delta ENT/\Delta ENT}$) the peripherally situated covernet fibrils, marginal band, Kimura's membrane and Hensen's stripe, and the striated sheet matrix within the core of the tectorial membrane, are all absent, indicating Tecta is an essential component of the non-collagenous tectorial membrane matrix[21]. The tectorial membrane of these *Tecta*$^{\Delta ENT/\Delta ENT}$ mice only contains randomly oriented collagen fibrils, and is completely detached from the surface of the organ of Corti. In the *Tectb*$^{-/-}$ mutant mice described in this study, the tectorial membrane remains attached to the organ of Corti but it lacks any sign of organised striated-sheet matrix within its core. Tecta is present within the tectorial membrane of these *Tectb*$^{-/-}$ mutant mice and disorganised, 8 nm diameter filaments can be seen in the matrix between the collagen fibril bundles, indicating that Tecta can, in the absence of Tectb, form filaments but is unable to form organised striated-sheet matrix. Tectb is therefore essential for formation of the striated-sheet matrix and may act as a cross-linker of Tecta-based filaments. Alternatively, Tectb may form homomeric filaments by virtue of its ZP domain[36], and these in turn may interact with Tecta-based filaments to form striated-sheet matrix.

The absence of Hensen's stripe in *Tectb*$^{-/-}$ mutant mice is striking. There is no evidence to suggest this structure is uniquely Tectb based but it is, however, formed during the later stages of postnatal development whilst the tectorial membrane is detaching from the surface of the receding greater epithelial ridge[37], in an area just above one of the three strips of cells that express the *Tectb* gene, a zone of cells in the greater epithelial ridge lying just medial to the IHCs[38]. A loss of the marginal band and a distinct enlargement of the tectorial membrane are observed in the apical end of the cochlea in *Tectb*$^{-/-}$ mutant mice. As yet undetected regional variations in the composition of the tectorial membrane matrix along its length may account for why the loss of Tectb has a more severe effect on the gross structure of the tectorial membrane in the apical, low-frequency region of the cochlea.

The mechanism by which forces are imparted to the hair bundles of the OHCs depends on the relationship between the radial stiffness of the tectorial membrane and the rotational stiffness of the OHC bundles[14, 19, 39]. The radial stiffness of the tectorial membrane has been attributed to the collagen fibril bundles that run radially across this matrix, although their contribution to the mechanical properties of the tectorial membrane has yet to be experimentally established[24, 39, 40]. The distribution of these collagen fibril bundles within the tectorial membrane in the high-frequency, basal end of the cochlea appears to be unaffected by the loss of Tectb, despite the loss of organisation in the surrounding matrix. Furthermore, extracellular receptor potentials recorded from OHCs in the 53 kHz region of the cochlea in response to tones of 10 kHz, a frequency at which excitation is stiffness dominated[2], are of similar magnitude, phase and symmetry in wild type and *Tectb*$^{-/-}$ mutant mice. The loss of Tectb and striated sheet matrix therefore has little, if any, influence on the dynamic radial stiffness of the tectorial membrane in the basal end of the cochlea. This conclusion is also supported indirectly by the CAP threshold audiograms. These depend

ultimately on the sensitivity of the OHCs, and are not significantly different in wild type and *Tectb*$^{-/-}$ mutant mice for frequencies above 20 kHz. In the apical, low-frequency region of the cochlea, the tectorial membrane is grossly enlarged and the marginal band is disrupted. This may prevent the tectorial membrane from properly engaging with the organ of Corti and stimulating the OHCs.

Tone-evoked BM vibrations measured at the 53 kHz place of *Tectb*$^{-/-}$ mice exhibit enhanced tuning; sensitivity at the tip of the tuning curve is largely preserved and the high- and low-frequency slopes either side of the tip are steeper than those in wild type mice, and the low-frequency tail of the tuning curve is relatively insensitive. Neural masking tuning curves recorded from *Tectb*$^{-/-}$ mutant mice have similar characteristics. They are similar in sensitivity, but are far sharper, with steeper high- and low-frequency slopes, than those recorded from wild type mice. Simultaneous neural masking relies on the non-linear, compressive, properties of the cochlea[5] and interactions between adjacent OHCs[41]. Thus the enhanced basilar membrane and neural frequency tuning recorded from *Tectb*$^{-/-}$ mutant mice can be attributed to a reduction in the spread of excitation along the BM and a diminished interaction between adjacent frequency regions in the cochlea.

Hensen's stripe has been attributed with a role in displacing the hair bundles of IHCs[28, 29]. Although this structural feature of the tectorial membrane is absent in *Tectb*$^{-/-}$ mutant mice, the CAP threshold audiograms and the neural masking tuning curves of wild type and *Tectb*$^{-/-}$ mutant mice are of similar sensitivity for tones greater than 20 kHz. Hensen's stripe is therefore not essential for exciting IHCs in the basal, high-frequency region of the mouse cochlea, at least at the characteristic frequency. It may, however, be important for exciting IHCs at frequencies away from the characteristic frequency, as the low-frequency tail of the neural tuning curve in *Tectb*$^{-/-}$ mutant mice is more insensitive, and the high- and low-frequency slopes are steeper than their counterparts in the basilar membrane mechanical tuning curves. Hensen's stripe may, therefore, have a role in coupling IHC hair bundles to fluid movements in the subtectorial space that are due to tones above or below their characteristic frequency.

The strong resonance that is evident 0.26 octaves below the tip of the basilar membrane threshold tuning curve in wild type mice has been attributed to the tectorial membrane [21, 22]. The resonance is not apparent as a separate peak in the basilar membrane tuning curves of *Tectb*$^{-/-}$ mutant mice, but is associated with a notch of insensitivity in the masking tuning curves where the tip of the tuning curve meets the tail[16, 22, 33, 42, 43]. The notch of insensitivity has been attributed to a minimum that would occur in the net shear between the tectorial membrane and reticular lamina if the radial motions of the reticular lamina and tectorial membrane were in phase at the resonance frequency of the tectorial membrane. At this frequency, the displacement of IHC hair bundles would be minimal[14, 16, 43]. In wild type mice, the notch of insensitivity is shifted closer to the tuning curve tip with increasing frequency, as was first observed for single unit recordings in the cat[16]. The notch is shifted considerably closer to the tip of the neural masking tuning curves of *Tectb*$^{-/-}$ mice, and follows the same frequency-dependent trend[16] of the tuning curve notches measured from wild type mice. An upward shift in the tectorial membrane resonance frequency could result from either a change in the coupling efficiency between the tectorial membrane and the OHC hair bundles, or a reduction in the acting mass of the tectorial membrane, the mass of the section of the tectorial membrane that responds to a particular frequency. As OHC extracellular receptor potentials are similar in wild type and *Tectb*$^{-/-}$ mutant mice for frequencies at which responses of the cochlear partition are stiffness limited, the stiffness of the coupling between the tectorial membrane and basilar membrane is unlikely to be changed by the loss of Tectb. An upward frequency shift of the tectorial membrane resonance can, therefore, be attributed to a reduction in the acting mass of the tectorial

membrane. The absence of a separate, clearly discernable tectorial membrane resonance from the vibrations of the basilar membrane is also reflected in the relative insensitivity of the basilar membrane tuning curve tail in *Tectb*$^{-/-}$ mutant mice for frequencies below the tip. The slope of this frequency region is 6 dB.octave^{-1} less in *Tectb*$^{-/-}$ mutant mice than it is in wild type mice, as would be expected if the frequency of the tectorial membrane resonance had been shifted closer to the peak. A 6 dB.octave^{-1} change in slope is also expected if the contribution of a single component (pole) in the form of the tectorial membrane resonance has been effectively removed from the tail of the cochlea's complex mechanical filter and inserted close to the characteristic frequency [13, 44]. The plots of the phase versus frequency of basilar membrane motion measured at the 53 kHz point, although having many properties in common with those obtained from other rodent species (Robles and Ruggero, 2001), are unusual in having a sharp phase reversal at frequencies close to that of the low-frequency resonance. These sharp phase changes are reminiscent of those associated with the sharp cochlear resonance measured from the sparsely innervated region of the mustached bat cochlea and have been attributed to standing waves[20, 43, 45]. The sharp phase change is shifted closer to the characteristic frequency of the 53 kHz place in *Tectb*$^{-/-}$ mutant mice and a separate low frequency resonance peak is not observed. It is possible that the tectorial membrane resonance interacts constructively with the basilar membrane in this frequency region, as has been proposed for the mustached bat[20], to enhance the frequency selectivity of the basilar membrane rather than being seen as a separate peak of sensitivity.

DPOAEs are only generated in the high-frequency regions of the cochlea at low sound pressure levels in *Tectb*$^{-/-}$ mutant mice, spreading to lower frequencies with increasing level of the primary tones (f1 and f2). This is further evidence that both the acting mass of the tectorial membrane and the spread of excitation along the length of the cochlea have been reduced by the loss of Tectb. As a consequence of reduced spread of excitation along the cochlea, higher levels of primaries are necessary to ensure that the responses of the OHCs can extend to adjacent regions of the cochlea to interact and generate DPOAEs[46]. The cochlea behaves as if a critical basilar membrane velocity has to be achieved in order to provide the shearing displacement between the tectorial membrane and reticular lamina that is necessary to excite the OHCs. Higher levels of the primary tones are required if the frequencies of the primary tones are reduced, as would be expected if the loss of Tectb causes an effective reduction in the acting mass of the tectorial membrane.

Conclusion

Enhanced frequency tuning and an attenuation in the spread of excitation along the length of the cochlea correlate with the loss of the striated-sheet matrix from the core of the tectorial membrane and an absence of Hensen's stripe. Whilst the absence of Hensen's stripe could account for the enhancement seen in the neural masker tuning curves, it is unlikely to account for enhanced basilar membrane tuning. It can be deduced, therefore, that the striated sheet matrix is required for mechanically coupling elements of the tectorial membrane along its longitudinal axis. Loss of the striated-sheet matrix and a reduction in the length of the tectorial membrane -OHC complex that responds to a particular frequency will cause a reduction in the acting mass of the tectorial membrane. It will also reduce the ability of OHCs in adjacent locations along the length of the cochlea to influence each other and, hence, to respond in synchrony to effectively amplify the cochlear vibrations. We therefore conclude that the tectorial membrane has a distinctive role in determining frequency resolution and the spread of excitation along the length of the cochlea.

METHODS

Gene targeting

Gene targeting in CCB embryonic stem cells was performed as described previously[6] using a targeting vector constructed with *Tectb* genomic clones isolated from a mouse genomic library (Stratagene). Two independently targeted ES cell lines were used to create germ line transmitting chimaeric mice by the injection of C57Bl6 blastocysts. Chimaeras were crossed with S129SvEv or C57Bl6 mice to produce heterozygous F1 progeny that were interbred to produce F2 mice on S129SvEv or mixed S129/C57 backgrounds. Both cell lines produced mice with an indistinguishable phenotype. All experiments described were performed with mice derived from one ES cell line. Chimaeras were also outbred on both CBA/Ca and C57Bl6 background and heterozygous F6 and F7 mice from these lines were crossed to produce mutants on a CBA/C57 F1 hybrid background. All mice were used before 3-4 months of age to avoid age related hearing loss known to be prevalent in many mouse strains.

Tectb expression

Total RNA was isolated from single cochleae of $Tectb^{+/+}$, $Tectb^{+/-}$ and $Tectb^{-/-}$ mice, first strand cDNA was synthesised and used in the PCR reaction with primers for products of 816 bp spanning exons 1 to 8 of the *Tectb* mRNA, and 557 bp spanning exons 7 to 10 of the *Tectb* mRNA. As a positive control a 615 bp product specific for *Tecta* mRNA was amplified from all three mice. Negative control reactions were performed with no reverse transcriptase and no cDNA. Total protein from the tectorial membranes of $Tectb^{+/+}$ and $Tectb^{-/-}$ mutant mice at P57 and the greater epithelial ridges of P2 mice were separated by SDS-PAGE and blotted with rabbit antiserum R7 raised to full-length, native chick β-tectorin[47].

Morphology

Animals were killed by cervical dislocation and cochleae were removed and placed in PBS for dissection. To aid fixative penetration, the oval and round windows were removed and a small hole through to the scala media was made at the apical end of each cochlea. A small volume of fixative (2.5% glutaraldehyde in 0.1 M sodium cacodylate, pH 7.2, containing 1% tannic acid) was pipetted directly through the windows and the apical opening, and then the entire cochlea was transferred into the same fixative for 2 hours. Following 3 washes in 0.1 M sodium cacodylate, cochleae were fixed in 1% osmium tetroxide in 0.1 M sodium cacodylate pH 7.2 for 1 hr and washed a further 3 times in 0.1 M sodium cacodylate. Cochleae were then decalcified in 0.5 M EDTA for 7 days at 4 °C, before dehydration in an ascending ethanol series and inclusion in Epon resin via propylene oxide as an intermediate. For light microscopy, 1 μm thick sections were taken and stained briefly in 1% Toluidin blue containing 1% borax. Inner ears from 9 homozygote, 8 heterozygote and 7 wild type animals on the mixed C57/S129 background ranging in age from P14 to P88 were examined by light microscopy. For transmission electron microscopy, 100 nm thick sections were cut, stained with lead citrate and uranyl acetate, and viewed in a Hitachi 7100 microscope equipped with a Gatan Ultrascan 1000 CCD digital camera capturing images at a resolution of 2048×2048 pixels. In addition, inner ears from 2 $Tectb^{+/+}$, 4 $Tectb^{+/-}$ and 4 $Tectb^{-/-}$ mice on the F1 hybrid backgrounds at ages ranging from P130-P158 were examined by light microscopy. For scanning electron microscopy, cochleae from 2 $Tectb^{+/+}$, 2 $Tectb^{+/-}$ and 5 $Tectb^{-/-}$ mice at P26 on the mixed C57/S129 background were fixed in 2.5% glutaraldehyde in 0.1 M sodium cacodylate for 1–2 h, washed in cacodylate buffer, trimmed to reveal the surface of the organ of Corti, dehydrated in ethanol, critical point dried from liquid CO_2 and sputter coated with gold. Specimens were examined in a Leica Leo scanning electron microscope.

Cryosections of cochleae were prepared using methods described previously[48]. Cochleae from mature mice were decalcified at 4 °C for 1 week prior to agar-embedding and sectioning. Primary rabbit antisera were used overnight at the following concentrations: anti-alpha-tectorin (serum R9[47], 1:1000), anti-beta-tectorin (serum R7[47], 1:100) and anti-otogelin (1:3000, a kind gift from C. Petit, Institut Pasteur, Paris). Primary antibodies were visualised using FITC-conjugated swine anti-rabbit antibodies at a dilution of 1:100 for 2-3 hours. All antibodies were diluted into TBS containing 10% heat-inactivated horse serum.

To view the gross structure of the fresh, unfixed tectorial membrane, cochleae were dissected in artificial endolypmh (140 mM KCl, 5 mM NaCl, 25 μM $CaCl_2$, 25 μM $MgCl_2$, 10 mM Hepes pH 7.2) to expose the organ of Corti and stained with 1% Alcian blue for 10 min. Following a brief rinse, tectorial membranes were removed with fine needles, mounted under a coverslip on a glass slide in a drop of artificial endolymph, and photographed with a 63x oil immersion objective, NA 1.4, using Nomarski interference contrast optics.

The cross-sectional area, radial width and thickness of the tectorial membrane were measured from Toluidin blue stained, 1 μm thick plastic mid-modiolar sections of the apical and basal coils of the cochlea, and from anti-Tecta stained immunofluorescence micrographs of the basal coil, using Photoshop. To determine the area, the profile of the tectorial membrane was outlined and the pixel number was counted. Radial width was measured by extending a straight line from the lip of the spiral limbus to the peripheral edge of the tectorial membrane. Height was measured across the thickest region of the tectorial membrane with a line extending perpendicular to the lower surface of the tectorial membrane. Data for the analysis of plastic sections were obtained from 7 $Tectb^{-/-}$ cochlea, 5 $Tectb^{+/-}$ and 2 $Tectb^{+/+}$ mice. Differences were not detected between $Tectb^{+/-}$ and $Tectb^{+/+}$ so the data from these animals were pooled and compared with those from $Tectb^{-/-}$ mice using Student's t-test. For the anti-Tecta stained cryosections, cochleae from 2 $Tectb^{+/-}$ and 4 $Tectb^{-/-}$ mice were analysed.

Physiology

Mice, normally < 3 months of age, were anaesthetized with ketamine (0.12 $mg.g^{-1}$ body weight i.p.) and xilazine (0.01 $mg.g^{-1}$ body weight i.p.) for nonsurgical procedures or with Urethane (ethyl carbamate, 2 $mg.g^{-1}$ body weight, i.p.) for surgical procedures. The animals were tracheotomized, and their core temperature was maintained at 38 °C. To measure basilar membrane displacements, extracellular receptor potentials, and CAPs, a caudal opening was made in the ventrolateral aspect of the right bulla to reveal the round window (Fig. 3a). DPOAEs measured before and after surgery indicate that the bulla of the mouse can be opened without loss of sensitivity. CAPs were measured from the round window membrane using pipettes filled with artificial perilymph with tip diameters of 50–100 microns (recording bandwidth > 30 kHz). Extracellular receptor potentials were recorded from the organ of Corti with pipettes pulled from thin-walled quartz tubing (Sutter Instrument Company) filled with 3 M KCl, resistance 15–20 MΩ, bandwidth 12–18 kHz with capacitance compensation (Fig. 3a). Signals were amplified with a recording bandwidth of DC–100 kHz.

Tone-evoked basilar membrane displacements were measured by focusing the beam of a self-mixing, laser-diode interferometer[21, 49] through the round window membrane to form a 20 μm spot on the center of the basilar membrane in the 50–61 kHz region of the cochlea (Fig. 3a). The interferometer was calibrated at each measurement location by vibrating the piezo stack, on which it was mounted, over a known range of displacements. Tone pulses (rise-fall times 1 ms) during basilar membrane measurements were generated with a Phillips PM 5193 programmable synthesizer and attenuated with digitally controlled attenuators. Voltage responses from the interferometer were measured with a two-channel lock-in

amplifier (Princeton 5210) and digitized at 250 kHz with a Data Translation 3010 data acquisition board, and the peak response was stored on a PC. Experimental control, data acquisition, and data analysis were performed using a PC with programs written in TestPoint (CEC).

Sound was delivered via a probe with its tip within 1 mm of the tympanic membrane and coupled to a closed acoustic system (Fig. 4a) comprising two MicroTech Gefell 1 inch MK102 microphones for delivering tones and a Bruel & Kjaer 3135 ¼ - inch microphone for monitoring sound pressure at the tympanum. The sound system was calibrated in situ for frequencies between 1–70 kHz using a measuring amplifier and known SPLs were expressed in dB SPL re 2×10^{-5} Pa. The position of the coupler was adjusted to minimize peaks and dips in the calibration curve. White noise and tone pulses with rise-fall times of 0.2 ms were synthesized by a Data Translation 3010 data acquisition board, attenuated, and used for sound system calibration and the measurement of electrical and acoustical cochlear responses. Data were digitized at 250 kHz and stored on a PC. To measure DPOAEs, primary tones were set to generate 2f1–f2 distortion products at frequencies between 1 and 50kHz. DPOAEs were measured for levels of f1 ranging from 10–80 dB SPL, with the levels of the f2 tone set 10 dB SPL below that of the f1 tone. DPOAE threshold curves were constructed from measurements of the level of the f2 tone that produced a 2f1–f2 DPOAE with a level of 0 dB SPL where the frequency ratio of f2:f1 was 1.23. System distortion during DPOAE measurements was 80 dB below the primary tone levels.

CAP tuning curves were derived from simultaneous tone-on-tone masking[29] using a 10 ms probe tone centered on a 40 ms masker tone. The probe tone was set to a level where a stable CAP appeared just above the recording noise floor. The frequency of the masker was set and its attenuation was adjusted until the probe tone CAP was suppressed. The masker frequency and level was noted, a new masker frequency was set, and the process repeated. In a second group of experiments the probe level was set to increasingly higher values to see how the CAP tuning curves varied with probe tone level.

All procedures involving animals were performed in accordance with UK Home Office regulations with approval from the local ethics committee.

Acknowledgments

We thank J. Hartley for the design and construction of electronic apparatus. This work is supported by grants from the Wellcome Trust, the MRC, EuroHear and the BBSRC. KL and GR made the mutant mice, RG and GR did the morphological analyses, VL, AL and IR did the physiology, IR and GR wrote the manuscript.

REFERENCES

1. von Bekesy, G. Experiments in Hearing. McGraw-Hill; New York: 1960.
2. Geisler, CD. From Sound to Synapse. Oxford Univ. Press; Oxford: 1998.
3. Goodyear RJ, Richardson GP. Extracellular matrices associated with the apical surfaces of sensory epithelia in the inner ear: molecular and structural diversity. J Neurobiol. 2002; 53:211–227.
4. Dallos, P. Overview, Cochlear Neurobiology. In: Dallos, P.; Popper, AN.; Fay, RR., editors. The cochlea. Springer; 1996. p. 1-43.
5. Robles L, Ruggero MA. Mechanics of the mammalian cochlea. Physiol. Rev. 2001; 81:1305–1352. [PubMed: 11427697]
6. Dallos P, Billone MC, Durrant JD, Wang C, Raynor S. Cochlear inner and outer hair cells, functional differences. Science. 1972; 177:356–8. [PubMed: 5035486]
7. Sellick PM, Russell IJ. The responses of inner hair cells to basilar membrane velocity during low frequency auditory stimulation in the guinea pig cochlea. Hear. Res. 1980; 2:439–446. [PubMed: 7410248]

8. Dallos P. Organ of Corti kinematics. J. Assoc. Res. Otolaryngol. 2003; 4:416–421. [PubMed: 14690059]
9. Nowotny M, Gummer AW. Nanomechanics of the subtectorial space caused by electromechanics of cochlear outer hair cells. Proc. Natl. Acad. Sci. U S A. 2006; 103:2120–2125. [PubMed: 16461888]
10. Fridberger A, Tomo I, Ulfendahl M, Boutet de Monvel J. Imaging hair cell transduction at the speed of sound, dynamic behavior of mammalian stereocilia. Proc. Natl. Acad. Sci. U. S. A. 2006; 103:1918–23. [PubMed: 16446441]
11. Freeman DM, Masaki K, McAllister AR, Wei JL, Weiss TF. Static material properties of the tectorial membrane: a summary. Hear. Res. 2003; 180:11–27. [PubMed: 12782349]
12. Allen JB. Cochlear micromechanics - a physical model of transduction. J. Acoust. Soc. Am. 1980; 68:1660–1670. [PubMed: 7462465]
13. Zwislocki JJ. Theory of cochlear mechanics. Hear. Res. 1980; 2:171–182. [PubMed: 6997254]
14. Zwislocki JJ. Analysis of cochlear mechanics. Hear. Res. 1986; 22:155–169. [PubMed: 3733537]
15. Brown AM, Gaskill SA, Williams DM. Mechanical filtering of sound in the inner ear. Proc. Roy. Soc. B. 1992; 250:29–34.
16. Allen JP, Fahey PF. A second cochlear-frequency map that correlates distortion product and neural tuning measurements. J. Acoust. Soc. Am. 1993; 94:809–816. [PubMed: 8370887]
17. Gummer AW, Hemmert W, Zenner HP. Resonant tectorial membrane motion in the inner ear: Its crucial role in frequency tuning. Proc. Natl. Acad. Sci. USA. 1996; 93:8727–8732. [PubMed: 8710939]
18. Hemmert WM, Zenner HP, Gummer AW. Three-dimensional motion of the organ of Corti. Biophys. J. 2000; 78:2285–2297. [PubMed: 10777727]
19. Kössl M, Russell IJ. Basilar membrane resonance in the cochlea of the moustached bat. Proc. Nat. Acad. Sci. 1995; 92:276–279. [PubMed: 7816832]
20. Russell IJ, Kössl M. Micromechanical responses to tones in the auditory fovea of the greater mustached bat's cochlea. J. Neurophysiol. 1999; 82:676–686. [PubMed: 10444665]
21. Legan PK, et al. A targeted deletion in α-tectorin reveals the tectorial membrane is required for the gain and timing of cochlear feedback. Neuron. 2000; 28:273–285. [PubMed: 11087000]
22. Legan PK, et al. A deafness mutation demonstrates a second role for the tectorial membrane in hearing. Nat. Neurosci. 2005; 8:1035–42. [PubMed: 15995703]
23. Naidu RC, Mountain DC. Measurements of the stiffness map challenge a basic tenet of cochlear theories. Hear. Res. 1998; 124:124–31. [PubMed: 9822910]
24. Freeman DM, Abnet CC, Hemmert W, Tsai BS, Weiss TF. Dynamic material properties of the tectorial membrane: a summary. Hear. Res. 2003a; 180:1–10. [PubMed: 12782348]
25. Chan DK, Hudspeth AJ. Mechanical responses of the organ of corti to acoustic and electrical stimulation *in vitro*. Biophys J. 2005; 89:4382–95. [PubMed: 16169985]
26. Hasko JA, Richardson GP. The ultrastructural organisation and properties of the mouse tectorial membrane matrix. Hear Res. 1988; 35:21–38. [PubMed: 2460426]
27. Simmler MC, Cohen-Salmon M, El-Amraoui A, Guillard L, Benichou JC, Petit C, Panthier JJ. Targeted disruption of otogelin results in deafness and severe imbalance. Nat Genet. 2000; 24:139–143. [PubMed: 10655058]
28. Crane HD. IHC-TM connect-disconnect and efferent control V. J. Acoust. Soc. Am. 1983; 72:93–101. [PubMed: 7108047]
29. Steele CR, Puria S. Force on inner hair cell cilia. Int. J. Solids. Struct. 2005; 42:5887–5904.
30. Müller M, von Hünerbein K, Hoidis S, Smolders JWT. A physiological place–frequency map of the cochlea in the CBA/J mouse. Hear. Res. 2005; 2002:63–73. [PubMed: 15811700]
31. Cheatham MA, Huynh KH, Gao J, Zuo J, Dallos P. Cochlear function in Prestin knockout mice. J Physiol. 2004; 560:821–30. [PubMed: 15319415]
32. Dallos P, Cheatham MA. Compound action potential (AP) tuning curves. J. Acoust. Soc. Am. 1976; 59:591–7. [PubMed: 1254787]
33. Taberner AM, Liberman MC. Response properties of single auditory nerve fibers in the mouse. J. Neurophysiol. 2005; 93:557–569. [PubMed: 15456804]

34. Ehret G, Moffat AJM. Noise masking of tone responses and critical ratios in single units of the mouse cochlear nerve and cochlear nucleus. Hear. Res. 1984; 14:45–57. [PubMed: 6746421]
35. Shera CA. Mechanisms of mammalian otoacoustic emission and their implications for the clinical utility of otoacoustic emissions. Ear Hear. 2004; 25:86–97. [PubMed: 15064654]
36. Jovine L, Oi H, Williams Z, Litscher E, Wassarman PM. The ZP domain is a conserved module for polymerization of extracellular proteins. Nat Cell Biol. 2002; 4:457–61. [PubMed: 12021773]
37. Rueda J, Cantos R, Lim DJ. Tectorial membrane-organ of Corti relationship during cochlear development. Anat Embryol (Berl). 1996; 194:501–14. [PubMed: 8905016]
38. Rau A, Legan PK, Richardson GP. Tectorin mRNA expression is spatially and temporally restricted during mouse inner ear development. J Comp Neurol. 1999; 405:271–80. [PubMed: 10023815]
39. Zwislocki JJ, Cefaratti LK. Tectorial membrane. II: Stiffness measurements in vivo. Hear Res. 1989; 42:211–27. [PubMed: 2606804]
40. Shoelson B, Dimitriadis EK, Cai H, Kachar B, Chadwick RS. Evidence and implications of inhomogeneity in tectorial membrane elasticity. Biophys J. 2004; 87:2768–77. [PubMed: 15454468]
41. Bonfils P, Remond MC, Pujol R. Efferent tracts and cochlear frequency selectivity. Hear Res. 1986; 24:277–83. [PubMed: 3793643]
42. Liberman MC, Dodds LW. Single-neuron labeling and chronic cochlear pathology. III. Stereocilia damage and alterations of threshold tuning curves. Hear. Res. 1984; 16:55–74. [PubMed: 6511673]
43. Lukashkin AN, Smith JK, Russell IJ. The tectorial membrane resonance: manifestations in the cochlear acoustical and neural responses. J. Acoust. Soc. Am. 2006 in press.
44. Zwislocki, JJ. Auditory Sound Transmission: An Autobiographical Perspective. Erlbaum; Mahwah, NJ: 2002.
45. Shera CA. Mammalian spontaneous otoacoustic emissions are amplitude-stabilized cochlear standing waves. J. Acoust. Soc. Am. 2003; 114:244–262. [PubMed: 12880039]
46. Gaskill SA, Brown AM. The behavior of the acoustic distortion product, 2f1-f2, from the human ear and its relation to auditory sensitivity. J. Acoust. Soc. Am. 1990; 88:821–39. [PubMed: 2212308]
47. Knipper M, Richardson G, Mack M, Müller M, Goodyear R, Limberger A, Rohbock K, Köpschall I, Zenner H-P, Zimmermann U. Thyroid hormone-deficient period prior to the onset of hearing is associated with reduced levels of β-tectorin protein in the tectorial membrane. J. Biol. Chem. 2001; 276:39046–39052. [PubMed: 11489885]
48. Goodyear R, Richardson G. Distribution of the 275 kD hair cell antigen and cell surface specialisations on auditory and vestibular hair bundles in the chicken inner ear. J. Comp. Neurol. 1992; 325:243–56. [PubMed: 1281174]
49. Lukashkin AN, Bashtanov ME, Russell IJ. A self-mixing laser-diode interferometer for measuring basilar membrane vibrations without opening the cochlea. J. Neurosci. Methods. 2005; 148:122–9. [PubMed: 15978669]

Europe PMC Funders Author Manuscripts

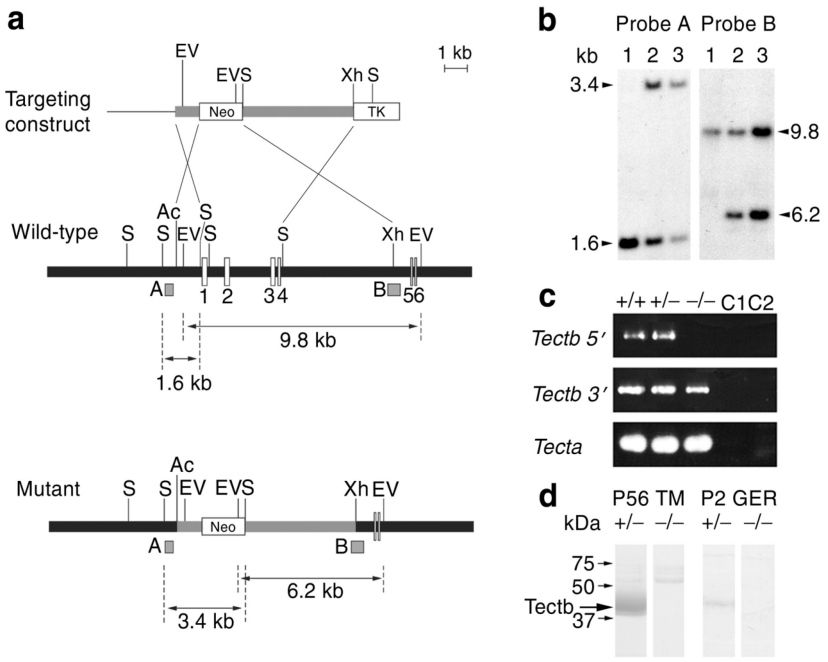

Figure 1.

Targeted deletion of exons 1–4 of *Tectb*. (**a**) Structure of the 5′ region of *Tectb*, the targeting vector and the targeted *Tectb* locus. Dark bars = genomic DNA; exons = open boxes; grey bar = homologous DNA in targeting vector; thin grey line = vector DNA. Lightly shaded boxes = external probes A and B; the sizes of the hybridising restriction fragments are shown. (Neo) Neomycin resistance gene; (TK) HSV thymidine kinase cassette; (S) *Sac*I; (EV), *Eco*RV; (Xh), *Xho*I; (Ac), *Acc*65I. (**b**) Southern blots of *Sac*I or *Eco*RV digested genomic DNA probed with external probes. (1) Wild type control: probe A hybridises to a 1.6 kb *Sac*I band, probe B hybridises to a 9.8 kb *Eco*RV band. (2, 3) Homologous recombinants: probes A and B hybridise to wild type bands, in addition probe A hybridises to a 3.4 kb *Sac*I band and probe B hybridises to a 6.2 kb *Eco*RV band. (**c**) RT-PCR of total RNA from $Tectb^{+/+}$ (+/+), $Tectb^{+/-}$ (+/–) and $Tectb^{-/-}$ (−/−) mice with primers for an 816 bp product spanning exons 1 to 8 of the *Tectb* mRNA (Tectb 5′), a 557 bp product spanning exons 7 to 10 of *Tectb* RNA (Tectb 3′), and a 615 bp product specific for *Tecta* (Tecta). C1, no reverse transcriptase control; C2, no cDNA control. (**d**) Western blots of P57 tectorial membranes and P2 cochlear epithelia from $Tectb^{+/+}$ (+/+) and $Tectb^{-/-}$ mutant (−/−) mice probed with anti chick β-tectorin. Arrow indicates the 45 kDa Tectb band.

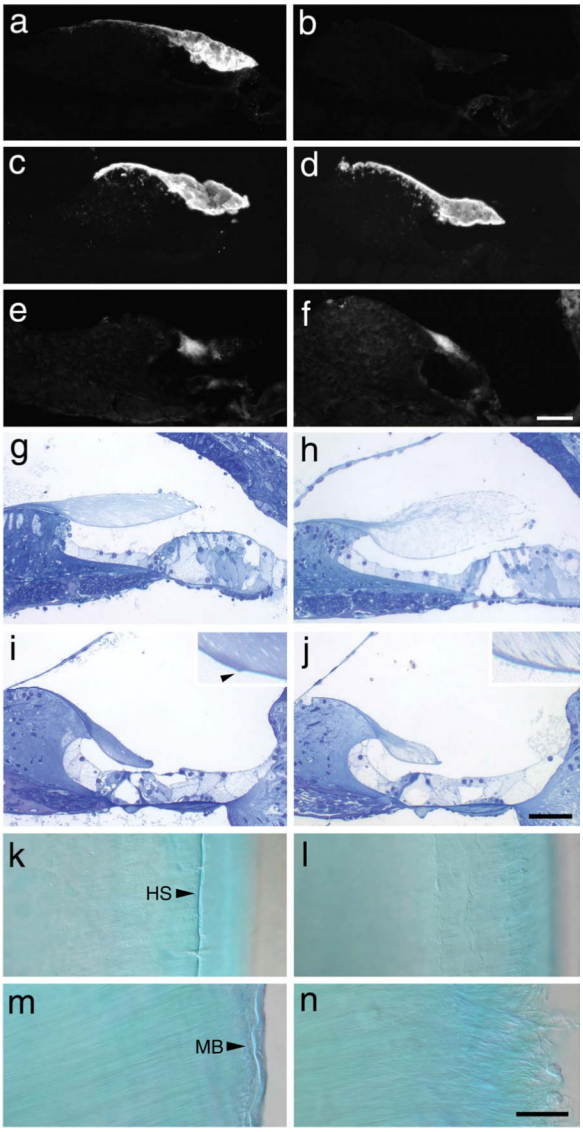

Figure 2.

Tectorial membrane morphology and composition in mature *Tectb*$^{+/-}$ and *Tectb*$^{-/-}$ mutant mice. (**a–f**) Cryosections from the basal coils of Tectb$^{+/-}$ (**a,c,e**) and *Tectb*$^{-/-}$ mutant (**b,d,f**) mice stained with antisera specific for Tectb (**a,b**), Tecta (**c,d**) and otogelin (**e,f**). The tectorial membranes from *Tectb*$^{-/-}$ mutant mice stain strongly for Tecta and otogelin but are negative for Tectb. (**g–j**) Toluidin blue stained sections from the apical (**g,h**) and basal (**i,j**) coils of the cochleae of adult *Tectb*$^{+/-}$ (**g,i**) and *Tectb*$^{-/-}$ (**h,j**) mice. Insets in **i** and **j** show a region of the lower surface of the tectorial membrane that lies just above the inner hair cells. Hensen's stripe is visible in **i** (arrowhead in inset). The tectorial membranes in *Tectb*$^{-/-}$ mice have a less dense structure compared to those of heterozygotes. (**k–n)** Wholemount preparations of Alcian blue stained tectorial membranes from *Tectb*$^{+/-}$ (**k,m**) and *Tectb*$^{-/-}$ (**l,n**) mice photographed with Nomarski interference contrast optics. (**k,l**) Basal region, HS = Hensen's stripe. (**m,n**) Apical region, MB = marginal band. Bar in **f** = 100 μm and applies to **a–f**, bar in **j** = 50 μm and applies to **g–j**, bar in **n** = 20 μm and applies to **k– n**.

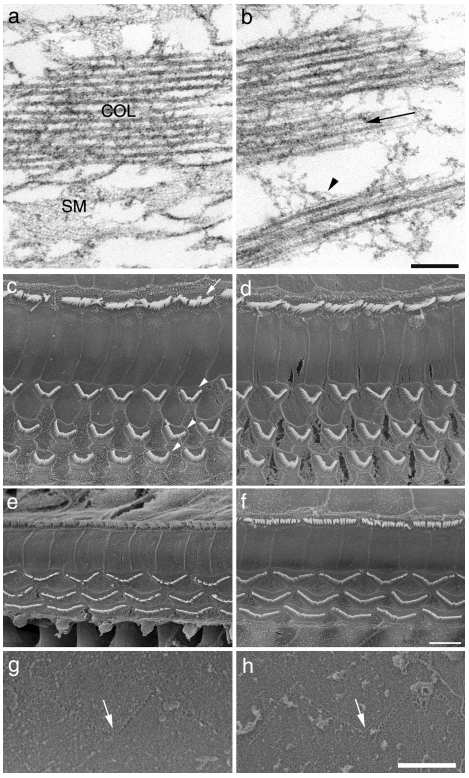

Figure 3.

Fine structure of the tectorial membrane and hair bundles. (**a,b**) Transmission electron micrographs of apical-coil tectorial membranes from adult *Tectb*$^{+/-}$ (**a**) and *Tectb*$^{-/-}$ (**b**) mice. In *Tectb*$^{+/-}$ mice (**a**), the tectorial membranes show the typical pattern of striated-sheet matrix (SM) and collagen fibrils (COL). In *Tectb*$^{-/-}$ mice (**b**), the tectorial membranes lack striated sheet matrix, and have irregular 8 nm diameter filaments (arrowheads) and straight filaments (arrow) between the collagen fibrils. (**c–f**) Scanning electron micrographs showing the apical surface of the organ of Corti in the apical (**c,d**) and basal (**e,f**) cochlear regions of *Tectb*$^{+/-}$ (**c,e**) and *Tectb*$^{-/-}$ mice (**d,f**). In panel **c**, the arrow indicates the single row of inner hair cell hair bundles, and the arrowheads indicate the three rows of outer hair cell hair bundles. (**g– h**) Scanning electron micrographs revealing the presence of OHC hair-bundle imprints (arrows) in the lower surface of the tectorial membranes of *Tectb*$^{+/-}$ (**g**) and *Tectb*$^{-/-}$ (**h**) mice. Bar in b = 200 nm and applies to **a**–**b**, bar in **f** = 5 μm and applies to **c**–**f**, bar in **h** = 2 μm and applies to **g**–**h**.

Europe PMC Funders Author Manuscripts

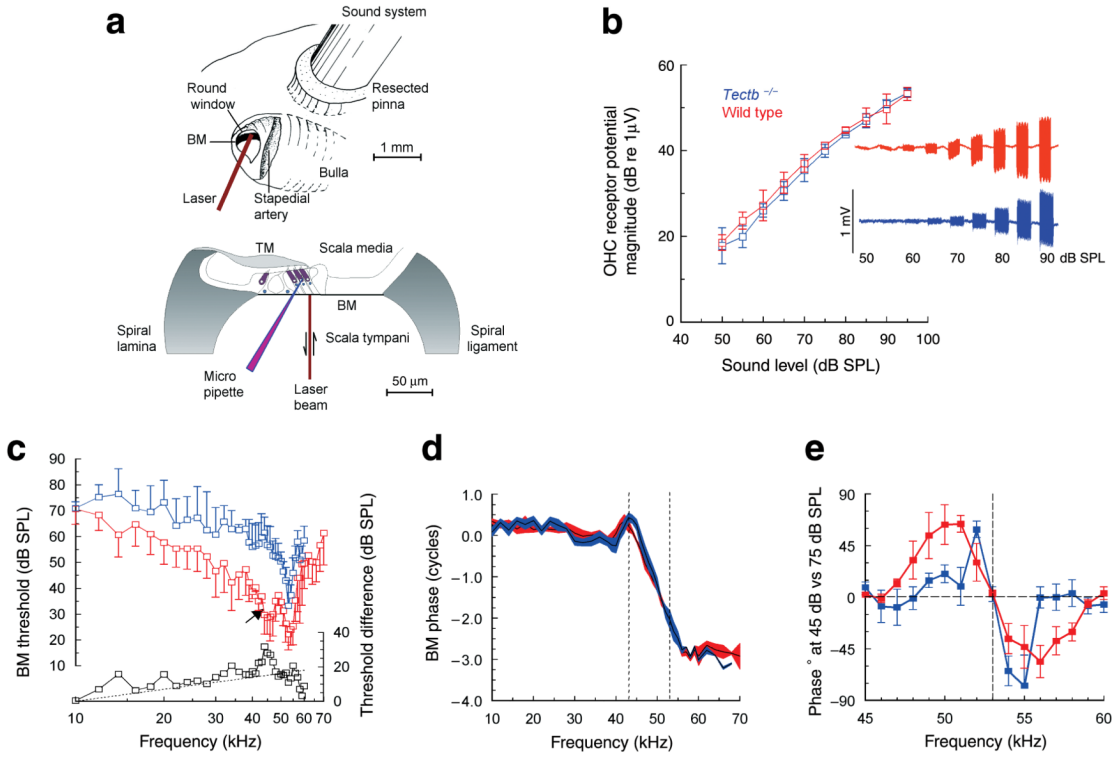

Figure 4.

Electrical and mechanical recordings from the cochleae of wild type (red) and *Tectb*$^{-/-}$ (blue) mice. (**a**) Set up for recording from the mouse cochlea. The round window is accessed via a caudal opening in the ventrolateral aspect of the bulla and the sound system probe tip is within 1 mm of the tympanum. Cochlear cross-section showing the organ of Corti, the tectorial (TM) and basilar (BM) membranes, the location of the recording pipette, and the laser diode beam used for measuring basilar membrane vibrations. (**b**) Magnitude and form of OHC extracellular receptor potentials in response to a 10 kHz tone as a function of level. Each record is an average of 10 presentations. (**c**) Iso-response displacement frequency tuning curves (mean ± s.d., n = 8 for each genotype) response criterion 0.2 nm, 53 kHz location). Arrow, low-frequency resonance. Black symbols: difference between wild type and *Tectb*$^{-/-}$ tuning curves. Dotted line, 6 dB.octave^{-1}. (**d**) The phases of basilar membrane (BM) responses (mean ± s.d., n = 4 for each genotype) to 70 dB SPL tones as a function of frequency. Vertical dashed lines indicate frequencies of the low-frequency resonance (43 kHz) and the characteristic frequency (CF) (53 kHz). (**e**) Phase difference (in degrees, mean ± s.d., n = 4 for each genotype) between basilar membrane displacements at 45 and 75 dB SPL. Zero crossing slopes: wild type 33.28° kHz^{-1}, *Tectb*$^{-/-}$ mice 61.75° kHz^{-1}.

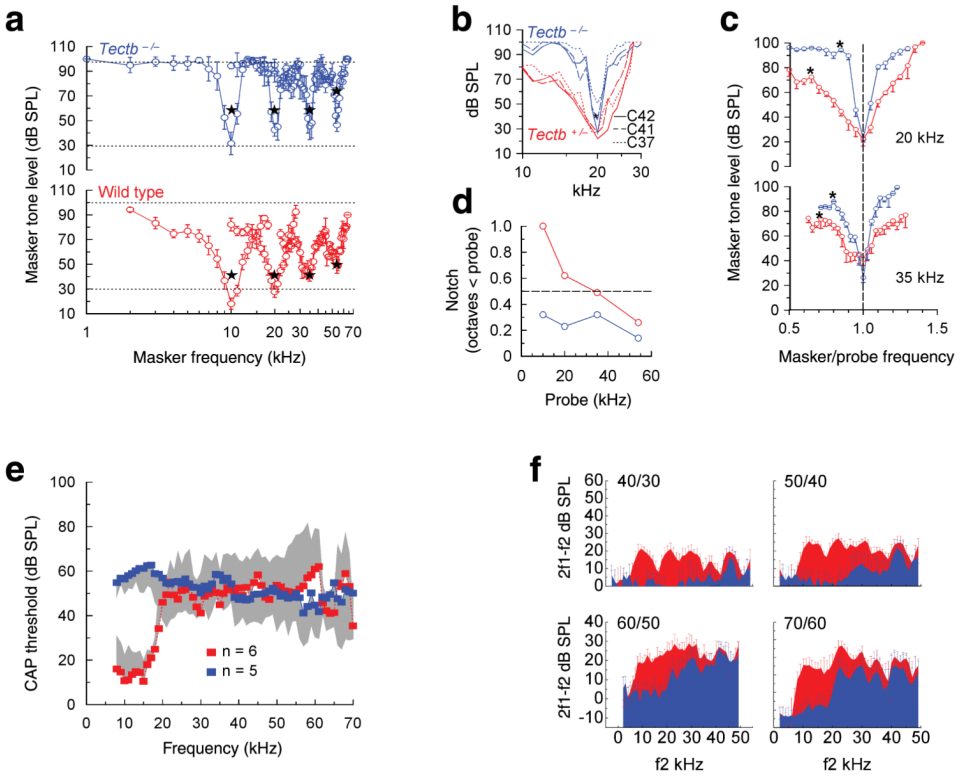

Figure 5.

Neural and acoustical recordings from the cochleae of wild type (red) and *Tectb*$^{-/-}$ (blue) mice. (**a**) Simultaneous masking tuning curves (n = 30, mean ± s.d) of compound action potentials in response to 10, 20, 35 and 54 kHz probe tones. The levels and frequencies of the probe tone are indicated by stars. Dotted lines indicate SPLs of 30 and 100 dB. (**b**) The means (n = 10) of masking tuning curves for a 20 kHz probe tone for individual mice from each of 3 different F1 hybrid families (C37:CBA/Ca f6 × C57/BL6 f5; C41: CBA/Ca f6 × 129SvEv; C42: C57/BL6 f7 × 129SvEv). (**c**) Neural masking tuning curves (n = 30 for each genotype) for 20 kHz (upper) and 35 kHz (lower) probe tones. Masker frequency is expressed as a ratio of the probe tone frequency, stars indicate the notches of insensitivity. (**d**) Notch frequency in octaves below the tuning curve tip-frequency as a function of probe-tone frequency. (**e**) Mean ± s.d. (n = 10) of the CAP detection threshold as a function of tone frequency. Grey shading indicates +s.d. of wild type and –s.d. of *Tectb*$^{-/-}$ data. (**f**) Mean ± s.d. (n =10) of the magnitude of 2f1–f2 DPOAEs as functions of f2 frequency. Levels of f2/f1 tones in dB SPL are shown in the upper left of each panel.

Europe PMC Funders Author Manuscripts

Europe PMC Funders Author Manuscripts

Table 1

Neural frequency tuning characteristics of wild type and *Tectb*$^{-/-}$ mutant mice

Probe Tone KHz	WT Q_{10dB}	*Tectb*$^{-/-}$ Q_{10dB}	WT LF Slope dB.octave^{-1}	*Tectb*$^{-/-}$ LF Slope dB.octave^{-1}	WT HF Slope dB.octave^{-1}	*Tectb*$^{-/-}$ HF Slope dB.octave^{-1}	WT Threshold dB SPL	*Tectb*$^{-/-}$ Threshold dB SPL
10	6.25	12.5	95 ± 6	140 ± 7	95 ± 3	150 ± 11	18.1 ± 4.5	31.6 ± 9.1
20	8.3	12.5	75 ± 8	335 ± 11	130 ± 4	285 ± 14	27.8 ± 4.5	42.6 ± 5.2
36	5.8	15.9	105 ± 3	280 ± 15	105 ± 6	402 ± 26	47.1 ± 7.1	45.7± 11.3
54	7.7	25.7	109 ± 5	513 ± 21	194.5 ± 8	513 ± 19	49.2 ± 4.5	46.6 ± 5.5

$Q_{10\ dB}$ (Bandwidth 10 dB from tip / characteristic frequency) as a function of probe tone frequency, low frequency (LF) and high frequency (HF) slopes of the tuning curve peaks, and neural suppression threshold at probe tone frequency for wild type (WT) and *Tectb*$^{-/-}$ mice. Data are shown as means ± standard deviations and are based on data shown in Fig. 4e.